

Experimental study of non-binary LDPC coding for long-haul coherent optical QPSK transmissions

Shaoliang Zhang,¹ Murat Arabaci,² Fatih Yaman,¹ Ivan B. Djordjevic,² Lei Xu,^{1,*} Ting Wang,¹ Yoshihisa Inada,³ Takaaki Ogata,³ Yasuhiro Aoki³

¹NEC Laboratories America, Inc., Princeton, NJ 08540, USA

²University of Arizona, ECE Department, 1230 E. Speedway Blvd., Tucson, AZ 85721, USA

³Submarine Network Division, NEC Corporation, 34-6, Shiba 5-chome, Minato-ku, Tokyo, 108-0014, Japan
leixu@nec-labs.com

Abstract: The performance of rate-0.8 4-ary LDPC code has been studied in a 50GHz-spaced 40Gb/s DWDM system with PDM-QPSK modulation. The net effective coding gain of 10dB is obtained at BER of 10^{-6} . With the aid of time-interleaving polarization multiplexing and MAP detection, 10,560km transmission over legacy dispersion managed fiber is achieved without any countable errors. The proposed nonbinary quasi-cyclic LDPC code achieves an uncoded BER threshold at 4×10^{-2} . Potential issues like phase ambiguity and coding length are also discussed when implementing LDPC in current coherent optical systems.

©2011 Optical Society of America

OCIS codes: (060.0060) Fiber optics and optical communications; (060.4080) Modulation; (999.9999) Low-density parity-check (LDPC) codes.

References and links

1. T. Kobayashi, A. Sano, H. Masuda, K. Ishihara, E. Yoshida, Y. Miyamoto, H. Yamazaki, and T. Yamada, "160-Gb/s Polarization-Multiplexed 16-QAM Long-Haul Transmission over 3,123 km Using Digital Coherent Receiver with Digital PLL Based Frequency Offset Compensator," in *Optical Fiber Communication Conference, OSA Technical Digest (CD)* (Optical Society of America, 2010), paper OTuD1.
2. D. Foursa, Y. Cai, J. Cai, C. Davidson, O. Sinkin, and B. Anderson, A. Lucero, A. Pilipetskii, G. Mohs, and N. Bergano, "Coherent 40 Gb/s Transmission with High Spectral Efficiency Over Transpacific Distance," in *Optical Fiber Communication Conference, OSA Technical Digest (CD)* (Optical Society of America, 2011), paper OMI4.
3. M. Salsi, C. Koebele, P. Tran, H. Mardoyan, E. Dutisseuil, and J. Renaudier, M. Bigot-Astruc, L. Provost, S. Richard, P. Sillard, S. Bigo, and G. Charlet, "Transmission of 96x100Gb/s with 23% Super-FEC Overhead over 11,680km, using Optical Spectral Engineering," in *Optical Fiber Communication Conference, OSA Technical Digest (CD)* (Optical Society of America, 2011), paper OMR2.
4. J. Cai, "100G Transoceanic Length Transmission with High Spectral Efficiency Using Bandwidth Constrained PDM-QPSK," in *Optical Fiber Communication Conference, OSA Technical Digest (CD)* (Optical Society of America, 2011), paper OMI3.
5. H. Sun, J. Gaudette, Y. Pan, M. O'Sullivan, K. Roberts, and K. Wu, "Modulation Formats for 100Gb/s Coherent Optical Systems," in *Optical Fiber Communication Conference, OSA Technical Digest (CD)* (Optical Society of America, 2009), paper OTuN1.
6. M. Scholten, T. Coe, and J. Dillard, "Continuously-Interleaved BCH (CIBCH) FEC Delivers Best in Class NECG for 40G and 100G Metro Applications", in *Optical Fiber Communication Conference, Technical Digest(CD)* (Optical Society of America, 2010), paper NTuB3.
7. M. Arabaci, Nonbinary-LDPC-Coded Modulation Schemes for High-Speed Optical Communication Networks," Ph.D. Dissertation, University of Arizona (2010).
8. I. B. Djordjevic, M. Arabaci, and L. L. Minkov, "Next generation FEC for high-capacity communication in optical transport networks," *J. Lightwave Technol.* **27**(16), 3518–3530 (2009).
9. D. Chang, F. Yu, Z. Xiao, Y. Li, N. Stojanovic, C. Xie, X. Shi, X. Xu, and Q. Xiong, "FPGA Verification of a Single QC-LDPC Code for 100 Gb/s Optical Systems without Error Floor down to BER of 10^{-15} ," in *Optical Fiber Communication Conference, OSA Technical Digest (CD)* (Optical Society of America, 2011), paper OTuN2.
10. K. Onohara, T. Sugihara, Y. Konishi, Y. Miyata, T. Inoue, S. Kametani, K. Sugihara, K. Kubo, H. Yoshida, and T. Mizuochoi, "Soft-secision-based forward error correction for 100 Gb/s transport systems," *IEEE J. Sel. Top. Quantum Electron.* **16**(5), 1258–1267 (2010).

11. I. B. Djordjevic, L. L. Minkov, L. Xu, and T. Wang, "Suppression of fiber nonlinearities and PMD in coded-modulation schemes with coherent detection by using Turbo equalization," *J. Opt. Commun. Netw.* **1**(6), 555–564 (2009).
12. S. Lin and D. J. Costello, Jr., *Error Control Coding: Fundamentals and Applications* (Prentice Hall, 2004).
13. M. C. Davey, "Error-correction using low-density parity-check codes," Ph.D. dissertation, University of Cambridge (1999).
14. J. G. Proakis, *Digital Communications* 4th ed. (New York: McGraw-Hill, 2000).
15. S. Zhang, X. Li, P. Y. Kam, C. Yu, and J. Chen, "Pilot-assisted, decision-aided, maximum likelihood phase estimation in coherent optical phase-modulated systems with nonlinear phase noise," *IEEE Photon. Technol. Lett.* **22**(6), 380–382 (2010).
16. J. Fu, M. Arabaci, I. B. Djordjevic, Y. Zhang, L. Xu, and T. Wang, "First Experimental Demonstration of Nonbinary LDPC-Coded Modulation Suitable for High-Speed Optical Communications," in *Optical Fiber Communication Conference*, OSA Technical Digest (CD) (Optical Society of America, 2011), paper OWF4.

1. Introduction

Exponentially-increasing Internet traffic growth has pushed the data rate requirements on optical communication systems to 40 Gb/s per channel and beyond. To meet this demand on high spectral efficiency (SE), multilevel modulation formats are potential solutions to upgrade existing optical networks from 10 Gb/s to higher bit rate per channel. However, to achieve a given bit error rate (BER) level with higher SE, higher-order modulation formats actually raises the required optical signal-to-noise ratio (OSNR) level by several times, thus leading to higher channel power. In addition to OSNR requirement, fiber nonlinearity would become another limiting factor on the maximum transmission distance. For instance, the longest distance reported so far for polarization-division-multiplexing (PDM) 16-quadrature amplitude modulation (QAM) is only 3,123 km operating at 160 Gb/s single-channel configuration [1]. In general, high-order QAM formats are only feasible for short-reach terrestrial systems. In contrast, quadrature phase-shift-keying (QPSK) with PDM techniques, capable of transmitting over transoceanic distance at 40 Gb/s [2] and even at 100 Gb/s [3], is one of the favorable modulation formats to support long-haul submarine optical communication [4], because of its OSNR receiver sensitivity and enhanced fiber nonlinearity tolerance [5].

In addition to the optimal modulation format, forward error correction (FEC) coding has been recognized as another powerful tool to ensure the maximum reach of data transmission at the minimal OSNR. FEC can be categorized into hard-decision and soft-decision decoding. Hard-decision decoder makes firm decisions on every input and output signals, such as Reed-Solomon (RS) and Bose-Chaudhuri-Hocquenghem (BCH) codes [6]. Since 1990s, RS codes have been widely deployed into contemporary optical systems and enhanced FEC codes have been intensively developed to further increase net coding gain (NCG). The 40Gb/s field-programmable gate array (FPGA) FEC encoder/decoder chip based on continuously-interleaved concatenated BCH (CI-BCH) was successfully implemented to achieve an NCG of 9.35 dB at 7% overhead [6], in bursty channel environment. In order to seek more than 10 dB NCG, researchers resort to soft-decision FEC codes and iterative decoding. Low-density parity-check (LDPC) codes are regarded as a superior class of FEC codes whose performances can approach the Shannon limit and whose decoders lend themselves to parallel implementation which is particularly important for optical fiber communications targeting ultra-high-speed bit rates [7].

Compared with binary LDPC, coded multilevel modulation schemes employing non-binary LDPC (NB-LDPC) codes as component codes have been shown to be promising advanced FEC candidates since they not only provide larger coding gains but also reduce latency at the receivers by avoiding costly turbo-equalization iterations [8]. The error-correction performance of LDPC codes have been evaluated through FPGA emulation [9,10] and transmission experiments [11]. The FPGA emulation is efficient in investigating BER floor that is frequently observed in LDPC decoding. Recently, just 20%-overhead binary quasi-cyclic LDPC (QC-LDPC) has been demonstrated to be error-floor-free down to coded BER of 10^{-15} using an FPGA emulator [9], which further confirms the high coding performances achievable via meticulous code design optimizations. In those emulated FPGA

decoders, only additive noise is taken into account without considering fiber nonlinearity or polarization convergence, which might make their evaluation results rather optimistic. Although experiment offline validation is quite difficult to demonstrate error-floor-free performance, which is vital for LDPC code design, such evaluation is a good complementary approach to evaluate the realistic performance of coding schemes in the presence of actual fiber impairments.

In this paper, the BER performance of NB-LDPC coded modulation schemes is studied in a digital coherent optical communication system, employing interleaved, PDM return-to-zero (RZ) QPSK signals. When a rate-0.8 (25% overhead) 4-ary QC-LDPC (69945,55956) code is employed, our scheme provides more than 10 dB coding gain at the BER of 10^{-6} for the back-to-back (B2B) case, and it achieves 10,560 km ultra-long-haul (ULH) transmission without any countable errors. To the best of our knowledge, this is the first experimental evaluation of a ULH wavelength-division-multiplexing (WDM) transmission over legacy dispersion managed fibers (DMFs) using a NB-LDPC code in a digital coherent communication system. We also discuss the implementation issue of LDPC coding, such as differential detection/decoding for resolving phase ambiguity and coding length.

2. Non-binary LDPC coded modulation

A q -ary LDPC code is given by the null-space of a sparse parity-check matrix defined over the finite field or Galois field of q elements, denoted $GF(q)$. An LDPC code is said to be (γ, ρ) -regular when the numbers of nonzero elements over all columns and over all rows of its parity-check matrix is equal to γ and ρ , respectively [12]. Otherwise, the LDPC code is called irregular. In order for a (γ, ρ) -regular LDPC code to be quasi-cyclic (QC), cyclically shifting any of its codewords by ρ positions must result in another codeword [12]. Quasi-cyclic LDPC (QC-LDPC) codes are an important class of LDPC codes due to being linear-time encodable and having a modular structure in their parity-check matrices which facilitates hardware implementation mainly by reducing routing complexity. LDPC codes are decoded using an iterative belief propagation algorithm commonly referred to as the sum-product algorithm (SPA). For decoding q -ary LDPC codes, an extension of SPA known as QSPA is used. Both QSPA and its fast Fourier transform (FFT) based implementation, denoted by FFT-QSPA, were first studied by Davey and MacKay [13]. When $q = 2^m$, m is an integer, i.e., when the LDPC code is defined over an extension of the binary field, FFT-QSPA becomes particularly attractive since the use of complex arithmetic is completely eliminated, and only real additions and subtractions are used. In this manuscript, we use 4-ary LDPC codes and employ FFT-QSPA in their decoding. Further details on how to construct non-binary QC-LDPC codes and their decoding can be found in [7] and references therein.

The use of bit-interleaved LDPC-coded modulation (BI-LDPC-CM) employing binary LDPC codes as component codes for addressing the high bit rate demands on ULH transmission links was discussed in our previous works [8,11]. As we have shown recently [7], however, non-binary LDPC coded modulation (NB-LDPC-CM) schemes outperform their counterpart BI-LDPC-CM schemes. Furthermore, when the order of the field over which the component NB-LDPC code is designed and the order of the modulation format are matched, NB-LDPC-CM eliminates the costly turbo-equalization iterations between the decoder and MAP detector, which are of critical importance for BI-LDPC-CM, and hence reduces the latency at the receivers while providing higher coding gains. In addition, when the underlying constellation sizes increase, both additional coding gains and computational savings offered by NB-LDPC-CM increase in comparison with BI-LDPC-CM. Therefore, as the transmission bit rates continue to increase, the underlying constellation sizes will continue to grow; consequently, these benefits of NB-LDPC-CM will render it as the ultimate coded modulation scheme for ULH transmission.

3. Experimental setup

We used the experimental setup shown in Fig. 1 to evaluate the performance of the NB-LDPC-CM schemes. In our experiments, we employed 4-ary LDPC codes as component

codes although our setup is generic and it can be applied to any 2^m -ary LDPC coded modulation scheme (m is a positive integer). The random sequence fed into the LDPC encoder was carefully selected to make sure that the distribution patterns are uniformly distributed. First, the 4-ary encoded sequence was split into two bit sequences according to the following symbol-to-bit mapping rule: $0 \rightarrow 00$, $1 \rightarrow 01$, $2 \rightarrow 10$, and $3 \rightarrow 11$. The two resultant bit sequences were differentially encoded and then uploaded into two 12.5 Gb/s pulse pattern generators. The I and Q arms were manually synchronized to ensure that the beginning of the LDPC bits from both PPGs occurs at the same time, thus making the received bits meaningful for LDPC decoder. The same output of IQ modulator is delayed by a few hundred symbols for decorrelation, and is polarization-multiplexed together to emulate PDM systems. This synchronization was also monitored through both sampling scope and offline digital signal processing (DSP) algorithm.

Four odd and four even wavelength channels are combined via a 50GHz/100GHz interleaver before being launched into the fiber. ECL was only used for testing channel and all other seven channels employed DFB lasers. The output of IQ modulator was carved into 50% RZ through MZM, and was then time-shifted by a half symbol period (20 ps) to generate time-interleaving PDM for enhancing fiber nonlinearity tolerance in DMF systems. In the transmission link, each loop consisted of 6 spans of 73km-long DMFs, resulting in total of ~ 800 ps/nm residual chromatic dispersion, which was compensated by a dispersion-compensating fiber (DCF) with +800ps/nm, leading to in total 480km per loop. Subsequently, two gain equalizers (GEQ) ensured a flat gain over all channels. Received signal power was kept at 1dBm throughout all the measurements.

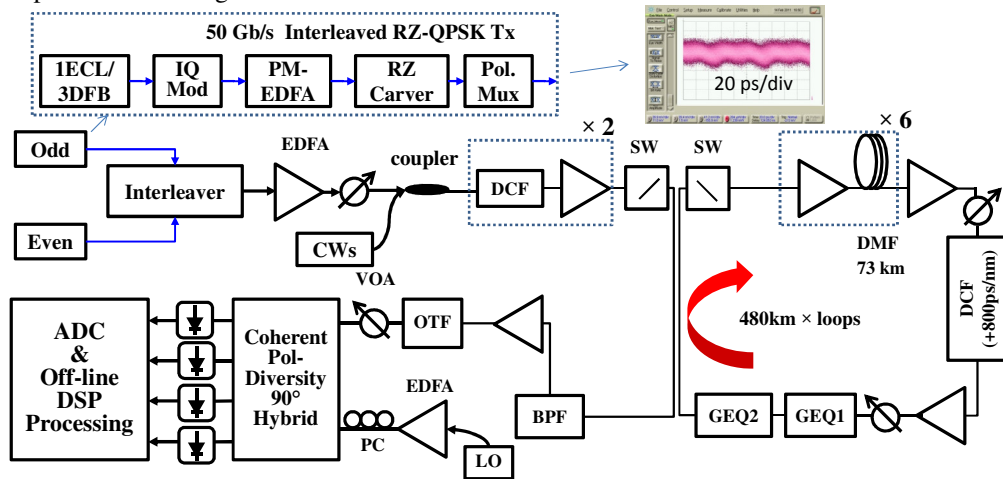


Fig. 1. Experimental setup for evaluating NB-LDPC. ADC: analog-to-digital converter. BPF: band-pass filter. DFB: distributed feedback laser, OTF: optical tunable filter. PC: polarization controller. SW: switch. VOA: variable optical attenuator. The inset shows the time-interleaved polarization-multiplexed RZ-QPSK waveform.

At the receiver side, a series of typical DSP algorithms were conducted, including re-sampling and polarization de-multiplexing. Following differential detection, the sampled sequences were passed to a MAP detector implementing sliding-window-based Bahl-Cocke-Jelinek-Raviv (BCJR) algorithm, referred to as SW-BCJR-MAP [11] and references thereof. By using the sliding-window-based implementation, we can run several MAP detectors of low complexity in parallel instead of running the BCJR algorithm over the whole received block, which becomes inhibitive as the block (or codeword) length increases. The symbol log-likelihood ratios (LLRs) calculated by the SW-BCJR-MAP detectors on each polarization branch are then input to corresponding 4-ary LDPC decoders as initial reliability estimates on codeword symbols (see Fig. 2). In our experiments, MAP detector depth was set to 128 symbols, and the 4-ary LDPC decoder was allowed to use 50 decoding iterations at the maximum. Further details on SW-BCJR-MAP and symbol LLR calculations can be found in

[7] and references therein. The 4-ary LDPC decoder enhances these initial reliability estimates through FFT-QSPA, and at the end of decoding, it provides the user with the final codeword estimates.

4. Results and discussion

4.1 Differential decoding versus differential detection

Differential encoding was used to avoid the phase ambiguity in the system because of phase noise and constant modulus algorithm (CMA) for separating the two orthogonal polarization states. At the receiver side, either differential decoding or differential detection can be performed to recover the original data. However, LDPC decoding requires the statistics information of the received signals to compute LLRs. As a result, we differentially detected the outputs of CMA, and then fed them into the LDPC decoding processor, consisting of an MAP detector and an NB-LDPC decoder, as depicted in Fig. 2. It is worth mentioning that the differential detection would bring additional 2~3 dB penalty compared to ideal coherent detection [14]. In our measured B2B BER results shown in Fig. 3, compared to differential decoding, about 2 dB OSNR penalty was observed at $\text{BER} = 10^{-3}$ by using differential detection. Of significance is that the penalty becomes smaller as BER goes higher since frequently-occurred errors would double the errors in both cases [14]. For instance, the penalty reduces to about 1 dB at $\text{BER} = 4 \times 10^{-2}$. This is the penalty we need to pay to avoid the potential burst errors from phase ambiguity.

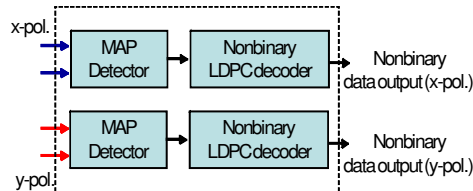


Fig. 2. Maximum a posteriori probability (MAP) detector and NB-LDPC decoder.

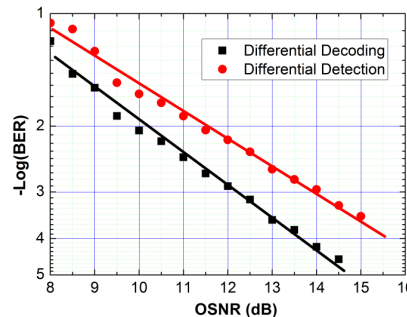


Fig. 3. B2B performance comparison between differential decoding and detection.

On the other hand, hard-decision FEC can be applied in differential decoding approach, in which hard symbol decision was made first before conducting different decoding. Unlike 2~3 dB penalty arising from differential detection, the penalty of differential decoding is only limited to ~0.5 dB penalty. It is expected that hard-decision FEC together with differential decoding is capable of achieving better coding gain than the scheme of soft-decision FEC with differential detection. It should be reminded that the coding gain of FEC is generally limited within 10 dB whereas soft-decision FEC is able to have more than 10 dB gain. In other words, given the same input OSNR, soft-decision FEC in differential detection case is most likely to have lower output BER than hard-decision FEC together with differential decoding.

The future work would focus on non-differential-encoded coherent systems with the aid of training data in order to mitigate phase cycle slips [15]. In those non-differential-encoded systems, soft-decision FEC would ensure the best coding gain performance.

4.2 Codeword length

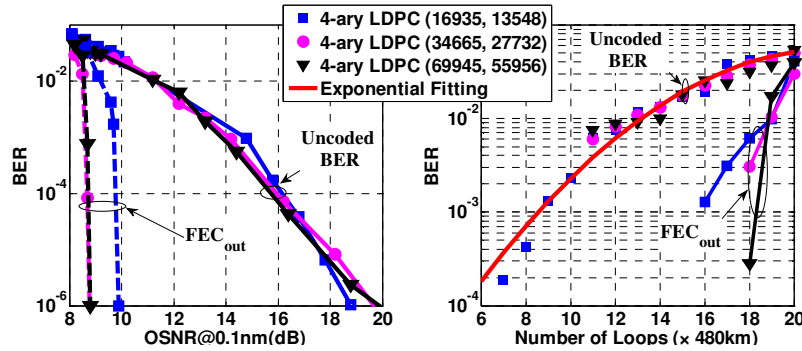


Fig. 4. Measured BER of B2B (a) and transmission (b) for three different rate-0.8, (3,15)-regular, 4-ary LDPC codes, namely LDPC(16935,13548), LDPC(34665,27732), and LDPC(69945,55956).

BER at each point was calculated from at least 40 million bits (averaging over 300 $4\mu\text{s}$ -long data sets). We also evaluated the performance of three different 4-ary quasi-cyclic LDPC codes in both B2B and transmission cases. Note that MAP was turned off here to speed up the decoding process and polarization states were time-aligned. The rate-0.8, (3,15)-regular, 4-ary LDPC(16935,13548) code of girth 8 provides about 9 dB coding gain at the BER of 10^{-6} [16]. The other two 4-ary, (3,15)-regular, rate-0.8 LDPC codes, namely LDPC (34665, 27732) and LDPC(69945,55956) codes, are both of girth 10 and they have longer codewords. Consequently, the latter two codes provide better error correction performance under the iterative LDPC decoding algorithm. As Fig. 4(a) indicates, the coding gain is further increased to >10 dB by using longer LDPC codes of girth 10. This observation is also found after loop transmission, as plotted in Fig. 4(b), where no countable errors were achieved after 17 loops using LDPC (34665, 27732) and LDPC(69945,55956) codes. In contrast, LDPC(16935,13548) only corrects all the bits error after 15 loops. In addition, based on Fig. 4, increasing the codeword length from 34665 to 69945 symbols, while maintaining the same girth, does not lead to any further improvement in the B2B BER performance though longer codeword is able to have a slightly better performance. Therefore, 4-ary LDPC (69945,55956) code was used for further experimental evaluation in time-interleaved manner with MAP detector. Note that the uncoded BER of LDPC (34665, 27732) and LDPC(69945,55956) below 11 loops were not plotted because no errors were observed after LDPC decoding between 11 loops and 18 loops.

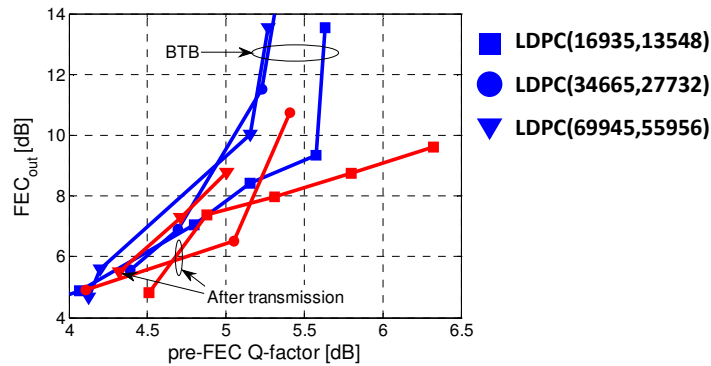


Fig. 5. The output Q-factor of three LDPC codes at BTB (blue lines) and after transmission (red lines).

To examine the impact of fiber nonlinearity on the LDPC decoder, we plot the FEC_out versus Q-factor graph where $Q[\text{dB}] = 20 \log_{10} \left(\sqrt{2} \text{erfc}^{-1} (2\text{BER}) \right)$ in Fig. 5. The LDPC codes with large girth are less affected by the fiber nonlinearity than shorter codes because of better error correction performance.

4.2 Transmission performance

Time-interleaving polarization multiplexing was used to investigate the potential maximum transmission reach of our system setup. Besides, MAP detector was deployed before the NB-LDPC decoder to further enhance its error correction capability. Figure 6 shows that the NB-LDPC-CM scheme is much less sensitive to launch power compared to uncoded case. Regardless of the origin of errors, i.e., random errors due to amplified spontaneous emission (ASE) noise or burst errors due to strong fiber nonlinearities (high launch power), the proposed NB-LDPC-CM scheme remains effective in correcting all the errors below its threshold. As shown in Fig. 7, the launch power per channel was set at -3.7 dBm, and the number of loops was swept from 5 up to 25 loops to determine the maximum transmission distance. As Fig. 7 indicates, the maximum transmission loops, without any countable error, is 22 loops, amounting to 10,560km. To our best knowledge, this is the first experimental evaluation of ULH WDM transmission over legacy DMF using a NB-LDPC code as the effective channel code.

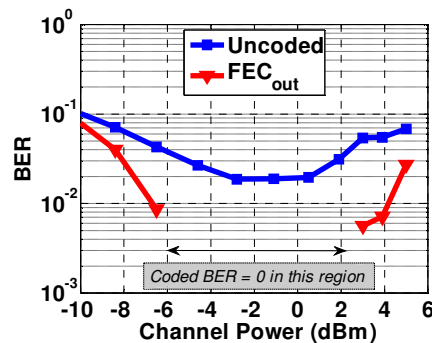


Fig. 6. Measured BERs for the uncoded case and for the 4-ary LDPC(69945,55956) coded modulation case after 20 loops at different launch powers.

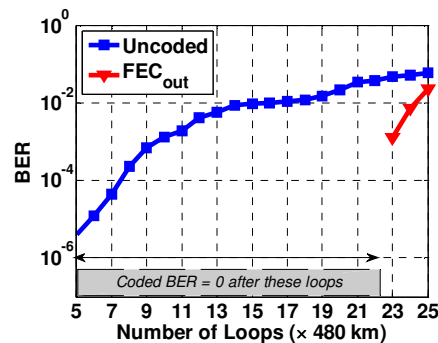


Fig. 7. Measured BERs for the uncoded case and for the 4-ary LDPC(69945,55956) coded modulation case versus the number of transmission loops when the launch power is -3.7 dBm.

5. Conclusion and future work

We studied the NB-LDPC-CM scheme in coherent optical communication systems, where the transmission reach over legacy DMF link, with the aid of time-interleaving polarization

multiplexing, can be increased to 10,560km without any countable error. The implementation issue like phase ambiguity and coding length has also been addressed in our experiments. Compared with the differential decoding approach, differential detection would lead to 1~3 dB gain loss depending on the FEC BER threshold. The future work will focus on how to remove the differential encoding in coherent optical systems and finally achieve the best coding gain performance.

The BER floor is difficult to predict by using simulation. That is why we emphasize the advantage of using real-time LDPC decoder to test the performance of LDPC codes, especially the error floor. Recently, concatenation of both hard-decision and soft-decision FEC is real-timely demonstrated to have a net coding gain up to 10.5 dB at the output BER level 10^{-15} [10]. However, with the proper design of LDPC codes, it is still possible to eliminate the BER error floor [9]. Therefore, although it may encounter error floor since we cannot demonstrate such a low BER using offline experiments, the potential benefits of nonbinary LDPC codes are very beneficial for optical transmission to further extend transmission reach.

Acknowledgments

The authors would like to thank Jiaojiao Fu from Zhejiang University for her help and useful discussions during this experiment. I. B. Djordjevic acknowledges support of NEC Labs and NSF under grant CCF-0952711.